Journal of Sound and Vibration (2000) **234**(3), 387–403
doi:10.1006/jsvi.1999.2880, available online at http://www.idealibrary.com on IDEAL®

VIBRATIONAL POWER FLOW INPUT AND TRANSMISSION IN A CIRCULAR CYLINDRICAL SHELL FILLED WITH FLUID

M. B. Xu

Department of Mechanical Engineering, The Hong Kong Polytechnic University, Hung Hom, Kowloon, Hong Kong

AND

W. H. Zhang

Department of Naval Architecture & Ocean Engineering, Huazhong University of Science and Technology, 430074 *Wuhan, Hubei, People's Republic of China*

(*Received* 21 *April* 1999, *and in final form* 30 *November* 1999)

In this paper, the characteristics of vibrational power flow in an infinite elastic circular cylindrical shell filled with fluid are investigated. The Flügge thin shell theory and Helmholtz equation are employed respectively in analyzing the wave motion in the shell wall and the sound field in the fluid. The coupling condition on the inner surface of the shell wall is introduced to obtain the vibrational equation of this coupled system. By using Fourier transform and its inverse transform, the input power into the coupled system excited by a driving force is studied. Along the shell axial direction, the transmission of the power flow carried by different internal forces of the shell wall and by the fluid is also studied. The results show that the input power flow and the power flow transmission depend mainly upon the characteristics of the free propagating waves in this coupled system.

1. INTRODUCTION

The vibration problem of fluid-filled shell systems is very important in many fields. The vibration not only causes the pollution of noise, but also affects the work of the devices which are mounted on the piping system. Hence, it is fundamental to investigate the characteristics of dynamic response of the fluid-filled shell system.

During recent years, a lot of attention has been paid to the coupled fluid–shell system. Merkulov *et al.* [1] considered the problem of excitation of normal modes by a point source located in the fluid contained in an elastic cylindrical shell. However, dispersion curves are limited to the real and imaginary planes and a relatively thick shell was presented for modes of circumferential order $n = 0$, 1, or 2. Merkulov *et al.* [2], proceeded to briefly study the point-force excitation of this shell–fluid coupled system. Their results are solely concerned with the relative transfer mobility of waves with varying branch and circumferential mode number; near-field effects at the source necessary for the calculation of the input mobility were not considered.

Fuller and Fahy [3] investigated the characteristics of free wave propagation in an infinite fluid-filled cylindrical shell. Their work was concerned with the solution and physical interpretation of the dispersion equation for the coupled system. Both dispersion

0022-460X/00/280387 + 17 $35.00/0

behavior and energy distribution of free waves were investigated. The distribution of vibrational energy between the shell wall and the fluid in the shell for free modes of propagation was obtained and its variation with frequency and material parameters was studied.

Pavic [4] gave the expression for the axial and the circumferential components of the unit energy flow along the shell wall in terms of the characteristic shell's components of the motion. He analyzed the influence of the three different terms contributing to the total energy flow and pointed out that the three terms exhibit considerable variations in contributing the total energy flow. Pavic [5] also investigated the wave motion and vibroacoustical energy flow through a fluid-filled pipe. The expressions of the energy flow in the wall and the fluid were given from the surface vibration and can be simplified at lower frequencies . Hence, the measurements of energy flow can be obtained by detection of surface vibrations only.

Based on Flügge's equation of motion and expressions for the total energy density in the shell, Williams [6] gave a rigorous derivation of the structural intensity for a thin cylindrical shell. The structural intensity vector is composed of five terms and simple physical interpretations of these five terms were presented in the article. A numerical model of a simply supported, point-driven, external fluid loading cylindrical shell existing in an infinite rigid baffle was studied.

Langley [7] studied the vibrational energy flow in a thin cylindrical shell, which is associated with helical wave motion. An approximate technique based on a well-known approximation to the dispersion relation was presented. A simple closed-form expression for the group velocity and the direction of the energy flow was given as a function of the helical wave angle by this method. The results show that the direction of the energy flow can differ significantly from the helical wave angle and a negative group velocity in the circumferential direction may arise in certain cases.

Fuller [8, 9] investigated the forced input mobility from an external force and the response due to an internal monopole source for a fluid-filled shell. However, the energy transmission along the shell axial direction was not given. Brevarts and Fuller [10] investigated further the effect of an internal flow on the dynamic behavior of an infinite elastic shell filled with fluid. The effect of upstream and downstream convections on the ratio of vibrational energy in the shell and fluid media for free waves was studied. Perhaps due to the complexity, the solution of the dispersion equation was limited to real roots for various circumferential mode numbers.

Zhang and Zhang [11, 12] studied the input vibrational power flow from an external force into a shell *in vacuo*. The power transmitted by different internal forces of the shell wall was derived and its variation with frequency and the shell axial distance was also studied.

James [13] studied the forced vibration of a fluid-filled pipe. The excitation considered in the paper was either an internal point source in the (contained) fluid or a mechanical point force located on the wall of the pipe. The acoustic power radiated into the exterior fluid, the vibration response of the shell wall, and the pressure in the exterior and interior fluids were calculated by a simple integration scheme. Numerical results were presented for the case of a water-filled steel pipe surrounded by air.

Feng [14] studied the acoustic properties of an infinite, fluid-filled shell. The relation between radiated sound power and the system power distribution for a single mode was analyzed in the paper. The results demonstrated that whether coupling with fluid increases or decreases the pipe response, and hence noise power, is largely dependent on the frequency range and on the way of excitation. Feng [15] found that there is a large discrepancy between lossless theory and experiments on vibration and noise levels of a water-filled elastic shell at high frequencies. This problem was investigated theoretically

and absorption due to the mixture layer on the inner wall of the shell was taken into account. The layer was treated as a special coupling layer with high damping, and the shell and the water were still treated as lossless. Numerical predictions were compared with the experimental measurements and good agreement was found.

Xu and Zhang [16] studied the forced vibrational power flow from a line circumferential cosine harmonic force into an infinite elastic circular cylindrical shell filled with fluid. An integrated numerical method along the pure imaginary axis of the complex wavenumber domain was used to analyze the response of the coupled shell–fluid system. Xu *et al.* [17] studied a fluid-filled cylindrical shell comprising a wall joint. The transmission loss through the wall joint was studied and an analysis of power flow transmission and reflection at the wall joint was presented. Xu *et al.* [18] considered an infinite cylindrical fluid-filled shell with periodic stiffeners. The input power flow from an external line force was studied and a periodic structural theory, space harmonic anlaysis was employed to investigate this fluid-coupled periodic structure. The influence of the parameters of the stiffeners upon the input power flow was discussed in this paper.

From the above, we can draw the conclusion that much attention has been paid to the free vibration of the fluid-filled shell system. As to force vibration, only the input power flow was given. The purpose of the present paper is to study further the forced vibrational power flow of an infinite elastic circular cylindrical shell filled with fluid. The Flügge thin-shell theory and the Helmholtz equation are employed respectively, in analyzing the wave motion in the shell wall and fluid contained in the shell. The vibrational equation is obtained by using the coupling condition of the shell–fluid system. The dynamic response of the coupled system to a circumferential line cosine harmonic force is derived and the results are obtained by using the method of residues. The vibrational power flow theory is introduced to study the dynamic response of this coupled system. In particular, the transmitted power flow along the shell axial direction carried by different internal forces (moment) of the shell wall and by the fluid will be analyzed, and its variation with frequency will also be discussed.

2. FREE WAVE PROPAGATION

Consider the free vibration behavior of an infinite circular cylindrical elastic shell filled with fluid. The co-ordinate system and the modal shapes are shown in Figure 1. The fluid is assumed to be viscous, isotropic and irrotational. The free, simple harmonic vibration of a thin-walled cylindrical shell is described by the Flügge thin-shell theory and the wave equation for the fluid is described by the Helmholtz equation [20, 22]

$$\sum_{i=1}^{3} L_{ij}(u, v, w) + f_j = 0, \quad j = 1, 2, 3, \tag{1}$$

$$\Delta p_f + k_0^2 p_f = 0, \tag{2}$$

where L_{ij} denote differential operators which are not explained here for the sake of brevity, f_j is the external load exerted on the shell in the direction of the co-ordinate axes and is given as

$$f_1 = f_2 = 0, \quad f_3 = D p_f, \tag{3}$$

$$D = R^2(1 - \mu^2)/(Eh). \tag{4}$$

Other symbols are given in Appendix A.

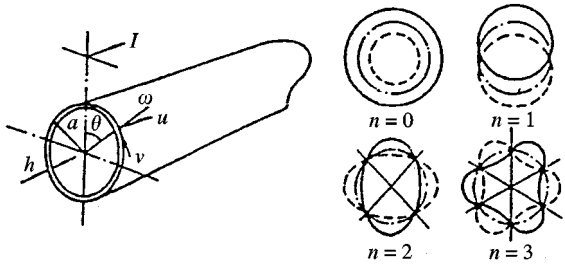

Figure 1. Coordinate system and modal shapes

The normal mode shapes assumed for the displacements of the shell wall and the pressure field in the contained fluid, associated with an axial wavenumber k_{ns}, are expressed as

$$[u \;\; v \;\; w \;\; p_f]^{\mathrm{T}} = \sum_{s=1}^{\infty} \sum_{n=0}^{\infty} \left(\left[U_{ns} \;\; V_{ns} \frac{\sin(n\theta)}{\cos(n\theta)} \;\; W_{ns} \;\; P_{ns} J_n(k_s^r r) \right]^{\mathrm{T}} \right) \cos(n\theta) \exp(\mathrm{i}\omega t + k_{ns} x) \quad (5)$$

Application of the fluid momentum equation at the shell wall, $r = R$, produces

$$P_{ns} = [\omega^2 \rho_f / k_s^r J_n'(k_s^r R)] W_{ns}. \quad (6)$$

where Jn( ) is Bessel function of order n [21].

Substitution of equations (5) and (6) into the shell equations results in the equations of motion of the coupled system, represented in matrix form as

$$[L_{3\times 3}][U_{ns} \;\; V_{ns} \;\; W_{ns}]^{\mathrm{T}} = [0 \;\; 0 \;\; 0]^{\mathrm{T}}, \quad (7)$$

where the elements of matrix $L_{3\times 3}$ are not given here for the sake of brevity.

The equations governing the motion of this coupled system differ from the *in vacuo* shell equations [11] by the presence of the fluid-loading term FL, which can be obtained from the boundary condition of the shell wall and is given by [3]

$$FL = \Omega^2 (\rho_f / \rho_s)(h/R)^{-1} (k_s^r R)^{-1} [J_n(k_s^r R) / J_n'(k_s^r R)]. \quad (8)$$

Expansion of the determinant of the amplitude coefficient in equations (7) provides the characteristic equation of this coupled system, expressed as

$$P_1(\lambda) + P_2(\lambda) FL = 0, \quad (9)$$

where both $P_1(\lambda)$ and $P_2(\lambda)$ are polynomials of λ. For the sake of brevity, the coefficients are not given here.

Due to the "non-linearity" of the characteristic equation, numerical methods have to be employed to find the desired eigenvalues k_{ns}. The eigenvalues will be either pure real, pure imaginary or complex. The pure real and imaginary roots can be found by the method of bisection. Newton's downhill method and plane grille searching method can be combined to find the complex roots.

Substituting the roots k_{ns} of the system's characteristic equation back into equation (7), the characteristic vectors ϕ_{ns} and φ_{ns} can easily be obtained, which are expressed as

$$\begin{cases} \Phi_{0s} = \dfrac{U_{0s}}{W_{0s}} \\ \Psi_{0s} = 0 \end{cases} \quad \text{for } n = 0, \quad (10a)$$

$$\begin{cases} \Phi_{ns} = \dfrac{U_{ns}}{W_{ns}} = \dfrac{L_{12}L_{23} - L_{13}L_{22}}{L_{11}L_{22} - L_{12}L_{21}} \\ \Psi_{ns} = \dfrac{V_{ns}}{W_{ns}} = \dfrac{L_{21}L_{13} - L_{11}L_{23}}{L_{11}L_{22} - L_{12}L_{21}} \end{cases} \quad \text{for } n > 0. \tag{10b}$$

The characteristic vectors Φ_{ns} and Ψ_{ns} characterize the particular type of the wave motion, giving the ratio of the longitudinal and circumferential displacements to the flexural displacement.

3. FORCED VIBRATION

We now analyze the response of the shell–fluid coupled system to an external line force, applied around the circumference at $x = 0$,

$$F(\theta, t) = F_0 \cos(n\theta)\delta(0)\exp(\mathrm{i}\omega t). \tag{11}$$

The forced vibration of the shell and the fluid are described as

$$\sum_{i=1}^{3} L_{ij}(u, v, w) + f_j = 0, \quad j = 1, 2, 3, \tag{12}$$

$$\Delta p_f + k_0^2 p_f = 0, \tag{13}$$

where

$$f_1 = f_2 = 0, \quad f_3 = D[p_f + F_0\delta(0)]. \tag{14}$$

Taking Fourier transform of equations (11, 12) and applying the boundary condition give

$$[L_{3\times 3}]\{\tilde{U} \;\; \tilde{V} \;\; \tilde{W}\}^{\mathrm{T}} = \{0, 0, \Omega^2 F_0/2\pi\rho_s h\omega^2\}^{\mathrm{T}}, \tag{15}$$

where $\tilde{U}$, $\tilde{V}$ and $\tilde{W}$ are the spectral displacements of the shell; the elements of matrix L are the same as those of the matrix in equation (7) and hence are not given here for brevity.

Let matrix I be the inverse of matrix L. Thus, the solution of equation (15) can be obtained as

$$\begin{bmatrix} \tilde{U} \\ \tilde{V} \\ \tilde{W} \end{bmatrix} = \begin{bmatrix} I_{11} & I_{12} & I_{13} \\ I_{21} & I_{22} & I_{23} \\ I_{31} & I_{32} & I_{33} \end{bmatrix} \begin{bmatrix} 0 \\ 0 \\ \Omega^2 F_0/(2\pi\rho_s h\omega^2) \end{bmatrix}, \tag{16a}$$

$$\begin{bmatrix} \tilde{U} \\ \tilde{V} \\ \tilde{W} \end{bmatrix} = \Omega^2 F_0/(2\pi\rho_s h\omega^2) \begin{bmatrix} I_{13} \\ I_{23} \\ I_{33} \end{bmatrix}, \tag{16b}$$

where the elements of matrix $I_{3\times 3}$ can be easily obtained in terms of the elements of matrix $L_{3\times 3}$ as

$$\begin{aligned} I_{13} &= (L_{12}L_{23} - L_{12}L_{31})/(\det|L|), \\ I_{23} &= (L_{12}L_{13} - L_{11}L_{32})/(\det|L|), \\ I_{33} &= (L_{11}L_{22} - L_{12}L_{21})/(\det|L|). \end{aligned} \tag{17}$$

Application of the inverse transform of equation (16) gives the shell displacements as

$$\begin{bmatrix} u(x) \\ v(x) \\ w(x) \end{bmatrix} = \frac{\Omega^2 F_0}{2\pi\rho_s h R\omega^2} \begin{bmatrix} \int_{-\infty}^{\infty} I_{13} \exp(k_{ns}x)\,\mathrm{d}(k_{ns}R) \\ \int_{-\infty}^{\infty} I_{23} \exp(k_{ns}x)\,\mathrm{d}(k_{ns}R) \\ \int_{-\infty}^{\infty} I_{33} \exp(k_{ns}x)\,\mathrm{d}(k_{ns}R) \end{bmatrix}. \tag{18}$$

Once the integrals in equation (18) are solved, the shell displacements can be easily obtained. The form of equations (17) means that the complex integrals in equation (18) can be obtained by using the method of residues. The poles contained in the contour will be at the locations of the roots of characteristic equation $\det|L| = 0$, i.e., the free wavenumbers discussed in section 2.

The complex integrals can be written as

$$\begin{bmatrix} \int_{-\infty}^{\infty} I_{13} \exp(k_{ns}x)\,\mathrm{d}(k_{ns}R) \\ \int_{-\infty}^{\infty} I_{23} \exp(k_{ns}x)\,\mathrm{d}(k_{ns}R) \\ \int_{-\infty}^{\infty} I_{33} \exp(k_{ns}x)\,\mathrm{d}(k_{ns}R) \end{bmatrix} = 2\pi\mathrm{i} \times \begin{bmatrix} \sum_{s=1}^{\infty} \mathrm{Re}\, s(I_{13})_s \exp(k_{ns}x) \\ \sum_{s=1}^{\infty} \mathrm{Re}\, s(I_{23})_s \exp(k_{ns}x) \\ \sum_{s=1}^{\infty} \mathrm{Re}\, s(I_{33})_s \exp(k_{ns}x) \end{bmatrix}. \tag{19}$$

The displacements of the shell wall can be obtained from equations (18, 19) and expressed as

$$\begin{bmatrix} u(x) \\ v(x) \\ w(x) \end{bmatrix} = \frac{\mathrm{i}\Omega^2 F_0}{\rho_s h R\omega^2} \times \begin{bmatrix} \sum_{s=1}^{\infty} \mathrm{Re}\, s(I_{13})_s \exp(k_{ns}x) \\ \sum_{s=1}^{\infty} \mathrm{Re}\, s(I_{23})_s \exp(k_{ns}x) \\ \sum_{s=1}^{\infty} \mathrm{Re}\, s(I_{33})_s \exp(k_{ns}x) \end{bmatrix}. \tag{20}$$

The radial displacement of the shell wall at $x = 0$ is

$$w(0) = \frac{\mathrm{i}\Omega^2 F_0}{\rho_s h R\omega^2} \sum_{s=1}^{\infty} \mathrm{Re}\, s(I_{33})_s. \tag{21}$$

In equations (20, 21), there are infinite poles, i.e., free wavenumbers, which have to be simplified. In the paper, all the propagating waves and attenuated standing waves are considered; as to near-field waves, only those with small wavenumbers are included. The characteristics of residues of different waves have been discussed in reference [20] and are not given here for the sake of brevity.

Once the displacements of the shell wall are obtained, the pressure of the fluid contained in the shell at any point (x, r, θ) can be easily solved from the fluid–shell coupling condition.

4. POWER FLOW INPUT AND TRANSMISSION

The noise control and vibration reduction method depends upon the nature of the vibration, and thus it is of prime importance to predict the characteristics of vibration

power flow. In this section, the forced vibration power flow input into the coupled system and transmission along the shell axial direction will be discussed.

4.1. VIBRATIONAL POWER FLOW INPUT

When an external line force $F(\theta, t) = F_0 \cos(n\theta)\delta(0)\exp(\mathrm{i}\omega t)$ is applied radially on the wall of the fluid-filled shell, the radial displacement of the shell wall at $x = 0$ can be obtained from equation (21). Then the input power flow from this driving force is defined as follows [11]:

$$P_{input} = \int_0^{2\pi} \frac{1}{2} \mathrm{Re}\{-\mathrm{i}\omega F_0 w(0)^*\} \cos^2(n\theta)\, R d\theta = R\frac{\eta_n \pi}{2} \mathrm{Re}\{-\mathrm{i}\omega F_0 w(x=0)^*\}, \quad (22)$$

where the asterisk denotes the complex conjugate, and

$$\eta_n = \begin{cases} 2, & n = 0, \\ 1, & n \neq 0. \end{cases}$$

The non-dimensional power flow is defined as

$$P' = \frac{PE}{F_0^2 \pi} \frac{\Omega}{\omega}. \quad (23)$$

4.2. INPUT POWER FLOW DUE TO A SINGLE PROPAGATING WAVE

In order to discuss the characteristics of different propagating waves, the input power flow due to a single propagating wave is investigated.

The radial displacement at $x = 0$ due to a single propagating wave is defined as

$$w(0)_s = \frac{\mathrm{i}\Omega^2 F_0}{\rho_s h R \omega^2} Re\, s(I_{33})_s. \quad (24)$$

Then the input power flow due to a single propagating wave is defined as

$$P_{input,S} = R\frac{\eta_n \pi}{2} \mathrm{Re}\{-\mathrm{i}\omega F_0 w(0)_s^*\}. \quad (25)$$

4.3. POWER FLOW TRANSMISSION ALONG THE SHELL AXIAL DIRECTION

When an external force is applied on the shell wall, the forced vibration waves will propagate in the shell–fluid coupled system, and thus the input power flow will also be transmitted along the shell axial direction. At any interfaces $x = L$, the shell displacements $u(x)$, $v(x)$, $w(x)$ and slope $\partial w(x)/\partial x$ of the shell wall can be solved from equation (20). Meanwhile, there will be four internal forces (moments) of the shell wall in the axial direction, which can be easily derived from Flügge's thin-shell theory [19]. These forces

(moments) can be written as the functions of the shell displacements and slope, expressed as

$$\begin{aligned} N(x) &= f_N\left[u(x), v(x), w(x), \frac{\partial w(x)}{\partial x}\right], \\ T(x) &= f_T\left[u(x), v(x), w(x), \frac{\partial w(x)}{\partial x}\right], \\ S(x) &= f_S\left[u(x), v(x), w(x), \frac{\partial w(x)}{\partial x}\right], \\ M(x) &= f_M\left[u(x), v(x), w(x), \frac{\partial w(x)}{\partial x}\right], \end{aligned} \tag{26}$$

where $N(x)$, $T(x)$, $S(x)$ and $M(x)$ are the axial force, torsional shear force, transverse shear force and bending moment in the x direction respectively.

In the section $x = L$ of the shell wall, the vibrational power flow transmitted by these forces (moment) are respectively expressed as

$$\begin{aligned} P(L)_N &= \frac{\eta_n \pi R}{2} \operatorname{Re}\{-\mathrm{i}\omega N(L) u(L)^*\}, \\ P(L)_T &= \frac{\eta_n \pi R}{2} \operatorname{Re}\{-\mathrm{i}\omega T(L) v(L)^*\}, \\ P(L)_S &= \frac{\eta_n \pi R}{2} \operatorname{Re}\{-\mathrm{i}\omega S(L) w(L)^*\}, \\ P(L)_M &= \frac{\eta_n \pi R}{2} \operatorname{Re}\left\{-\mathrm{i}\omega M(L)\left(\frac{\partial w(L)}{\partial x}\right)^*\right\}. \end{aligned} \tag{27}$$

The total vibrational power flow in the shell wall is the sum of the power flow carried by these shell internal forces (moment) and expressed as

$$P(L)_{Shell} = P(L)_N + P(L)_T + P(L)_S + P(L)_M. \tag{28}$$

The vibrational power flow carried by the fluid P_{Fluid} will be obtained from the vibrational power flow in the shell wall. The total power flow of the system P_{total} at $x = L$ is the sum of the power flow carried by the shell wall and by the fluid, that is

$$P_{total} = P(L)_{Shell} + P(L)_{Fluid}. \tag{29}$$

Thus,

$$P(L)_{Fluid} = P_{total} - P(L)_{Shell}. \tag{30}$$

According to symmetry, as the forced power flow is input into this coupled shell–fluid system, half of the input power will be transmitted in the positive direction of the shell axial and the other half will be transmitted in the negative direction. Thus, the total power of the system at the section $x = L$ is

$$P_{total} = 0{\cdot}5\, P_{input}. \tag{31}$$

From equations (30) and (31), the vibrational power flow carried by the contained fluid P_{Fluid} can be obtained as

$$P(L)_{Fluid} = 0{\cdot}5\, P_{input} - P(L)_{Shell}. \tag{32}$$

Once these types of vibrational power flow are given, the ratios of the power flow carried by different shell internal forces (moment) to the total power in the shell wall can be obtained, and thus the characteristics of shell motion will be interpreted from the point of energy. Meanwhile, the degree to which the energy is concentrated in the contained fluid or in the shell wall can also be analyzed in the same manner.

5. RESULTS AND DISCUSSIONS

A cylindrical shell filled with fluid will be considered as a numerical example model. The following parameters of this coupled shell are used in the calculations: $h/R = 0{\cdot}05$, $\mu = 0{\cdot}3$, $\rho_s = 7800\ \text{kg/m}^3$ and $E = 1{\cdot}92 \times 10^{11}\ \text{N/m}^2$; the fluid has the density $\rho_f = 1000\ \text{kg/m}^3$.

5.1. VIBRATIONAL POWER FLOW INPUT

The fluid-filled shell is excited by a line circumferential cosine harmonic force of circumferential mode order $n = 0$, 1, 2 and 3. Figure 2 shows the non-dimensional input power flow P'_{input} plotted against non-dimensional frequency Ω. In order to investigate the influences of the contained fluid, the results for the same shell vibrating *in vacuo* are also plotted.

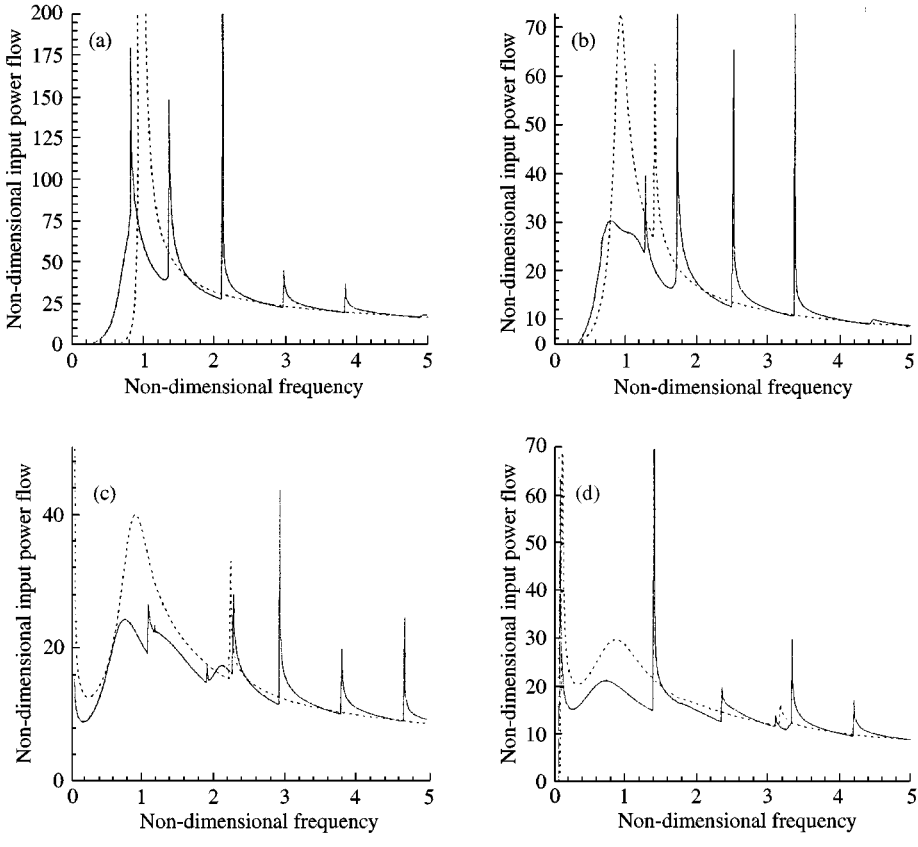

Figure 2. Non-dimensional input power flow into a shell: (a) $n = 0$, (b) $n = 1$, (c) $n = 2$, (d) $n = 3$. —— , Water-filled shell; ----------, shell *in vacuo*.

From the results in Figure 2 and the dispersion curves in reference [3], the following conclusions can be drawn. When $n = 0$, the existence of the fluid increases the input power flow into the coupled system at low frequencies ($\Omega < 1{\cdot}0$). The reason can be obtained from the characteristics of the free vibrational propagating waves. For the fluid-filled shell, there are two propagating waves, one of which corresponds to the fluid wave in a rigid-walled duct, the other to the extensional wave in the shell *in vacuo*. For the shell *in vacuo*, there exists only the propagating wave, the motion of which is mainly in the axial direction, while the external force is applied in the radial direction. Thus, the fluid contained in the shell has the effect of increasing the input power in these circumstances.

When $n > 0$, at low frequencies ($\Omega < 0{\cdot}7$), the difference in input power between fluid-filled shell and a shell *in vacuo* is negligible. The reason for this is that in a fluid-filled shell, there exists only one propagating wave, which corresponds to the propagating wave in a shell *in vacuo*. Thus, the effect of the fluid on the input power is insignificant in this condition.

At middle frequencies ($1{\cdot}0 < \Omega < 2{\cdot}0$), to any circumferential mode orders, the result for a shell *in vacuo* is much larger than that for a fluid-filled shell. The reason is that the shell *in vacuo* vibrates resonantly with the external force, while the fluid contained in the shell has the effect of reducing the resonant response.

At high frequencies ($\Omega > 2{\cdot}0$), for any circumferential mode orders, the difference in input power flow between a shell filled with fluid and a shell *in vacuo* is negligible except in frequency ranges near the peaks. Furthermore, the results for different circumferential mode orders are almost the same.

By comparing the input power with the dispersion curves, it is found that the frequencies of the peaks in the input power curve correspond to the cut-on frequencies of the propagating waves in the dispersion curves. When circumferential mode order n is large, because there are no propagating waves in the coupled system at low frequencies, the power flow is not input into the system by the external force.

In order to investigate the effect of the attenuated standing waves and the near-field waves on the input power flow, the complex integral in equation (18) is calculated only by using the residues of propagating waves. The results agree well with those calculated by the residues of all waves. In fact, the near-field waves only affect the phase of the displacements at the driving place, and so they do not have an effect on the results of input power flow. The attenuated standing waves always exist in pairs, one of which increases the input power, while the other decreases it, and so a pair of attenuated standing waves does not change the input power flow at all.

5.2. INPUT POWER FLOW DUE TO A SINGLE PROPAGATING WAVE

Figure 3 shows the non-dimensional input power flow due to a single propagating wave into a shell filled with fluid P'_s plotted against non-dimensional frequency Ω. From the results and the dispersion curves, the following conclusions can be drawn.

When $n = 0$, the input power due to the $s = 1$ propagating wave (cut-on frequency is $\Omega_{s=1} = 0$) $P'_{s=1}$ is almost the total power flow is the entire frequency-range. Moreover, $P'_{s=1}$ has a peak at the third propagating wave's cut-on frequency $\Omega_{s=3}$, which is just the peak of the whole power flow curves. At low frequencies, the power flow corresponding to the $s = 2$ wave (cut-on frequency is $\Omega_{s=2} = 0$) $P'_{s=2}$ is very small. With an increase in frequency, $P'_{s=2}$ will increase. Near the cut-on frequency of the third wave $\Omega_{s=3}$, $P'_{s=2}$ has a peak. After the peak, $P'_{s=2}$ will decrease with the increase in frequency. The power flow corresponding to the $s = 3$ wave (cut-on frequency $\Omega_{s=3} \neq 0$) $P'_{s=3}$ has two peaks: one

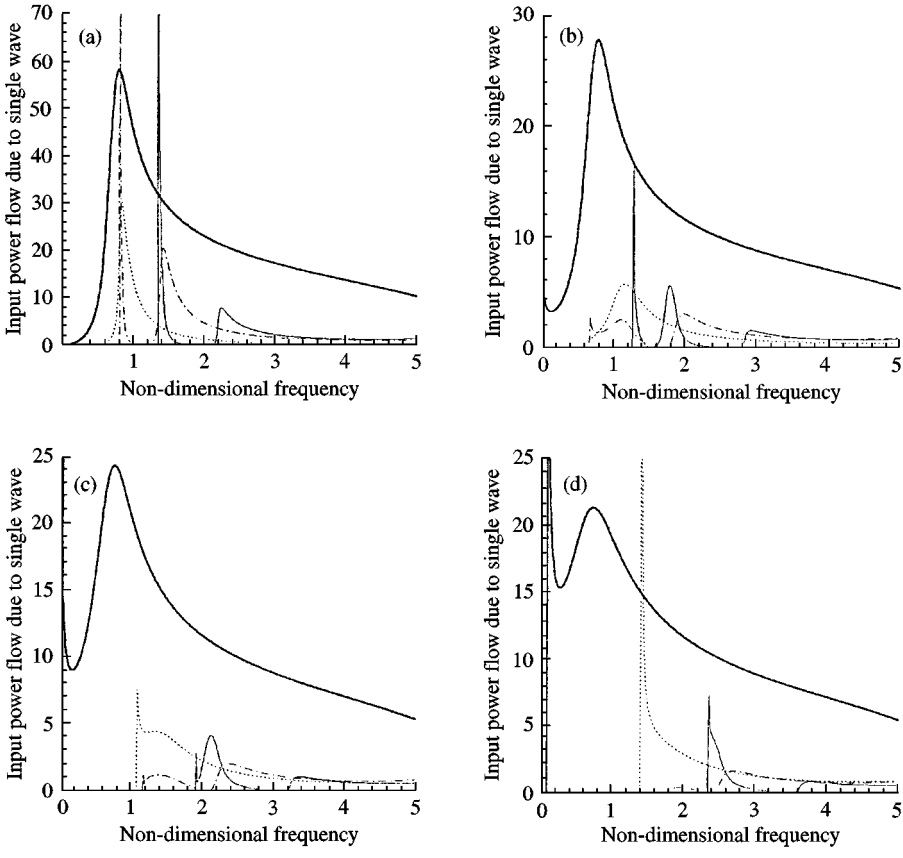

Figure 3. Input power flow due to a single propagating wave into a fluid-filled shell: (a) $n = 0$, (b) $n = 1$, (c) $n = 2$, (d) $n = 3$. ——, $s = 1$; ·····, $s = 2$; – · – · –, $s = 3$; ——, $s = 4$.

corresponds to $\Omega_{s=3}$ and the other corresponds to $\Omega_{s=4}$. Apart from the frequencies near the peaks, $P'_{s=3}$ is almost unnoticeable. The characteristics of the input power flow due to the propagating waves $s = 4, 5, 6, \ldots$ are similar to those of the wave $s = 3$.

The reason for the characteristics of the input power flow is given as follows. At low frequencies, the wave $s = 1$ is close to a fluid wave in a rigid-walled tube, which moves mainly in the radial direction; hence its input power flow is big. Moreover, the type of the wave motion changes near $\Omega_{s=2}$, which corresponds to the peak of the input power $P'_{s=1}$. The motion of the wave $s = 2$ is mainly in the axial direction at low frequencies, which makes the input power $P'_{s=2}$ very small. Near the frequency $\Omega_{s=3}$, the motion of the wave $s = 2$ changes into the motion in the radial direction to a great extent, and so $P'_{s=2}$ has a peak at $\Omega_{s=3}$. The character of the wave $s = 3$ changes quickly near its own cut-on frequency $\Omega_{s=3}$ and the next wave's cut-on frequency $\Omega_{s=4}$, and so the input power flow corresponding to the $s = 3$ wave $P'_{s=3}$ has two peaks just near these frequencies.

The results for $n > 0$ are similar to those for $n = 0$ except some small differences. The input power flow due to the waves $s = 3, 4, 5 \ldots$ has three peaks. For instance, the input power flow corresponding to the $s = 3$ wave $P'_{s=3}$ has three peaks at its own cut-on frequency $\Omega_{s=3}$, the next two waves' cut-on frequency $\Omega_{s=4}$ and $\Omega_{s=5}$. Apart from these three frequency ranges, $P'_{s=3}$ is unnoticeable. The reason for the results is that the motion of the wave changes greatly near these three frequencies.

The results for a shell vibrating *in vacuo* are similar to those of a shell filled with fluid. The input power due to the wave $s = 1$ is the main part of the whole power, while the input power due to the wave $s = 2, 3$ is insignificant except the regions near the propagating waves' cut-on frequencies. The results are shown in Figure 4.

5.3. POWER FLOW TRANSMISSION ALONG THE SHELL AXIAL DIRECTION

The vibration power flow transmission along the axial direction will be discussed in the section. The variations of $P'_{Shell} = P_{Shell}/P_{total}$, $P'_{Fluid} = P_{Fluid}/P_{total}$ and the variations of $P'_N = P_N/P_{Shell}$, $P'_T = P_Y/P_{Shell}$, $P'_S = P_S/P'_{Shell}$, $P'_M = P_M/P_{Shell}$ with non-dimensional distance L/R are investigated for different circumferential mode orders n and different non-dimensional frequencies Ω.

Figure 5 shows different power flows in the coupled system, P'_{Shell} and P'_{Fluid}, plotted against shell axial distance L/R for a fluid-filled shell. The following conclusions can be drawn.

At the driving point $L/R = 0$, for any circumferential mode order n and non-dimensional frequencies Ω, $P'_{Shell} = 1$ and $P'_{Fluid} = 0$. When L/R increases, P'_{Shell} will change to P'_{Fluid}.

At low frequencies ($\Omega = 0{\cdot}3$), the variations of P'_{Shell} and P'_{Fluid} are slow. For circumferential mode order $n = 0$, $P'_{Shell} \ll P'_{Fluid}$. The reason is that the only important

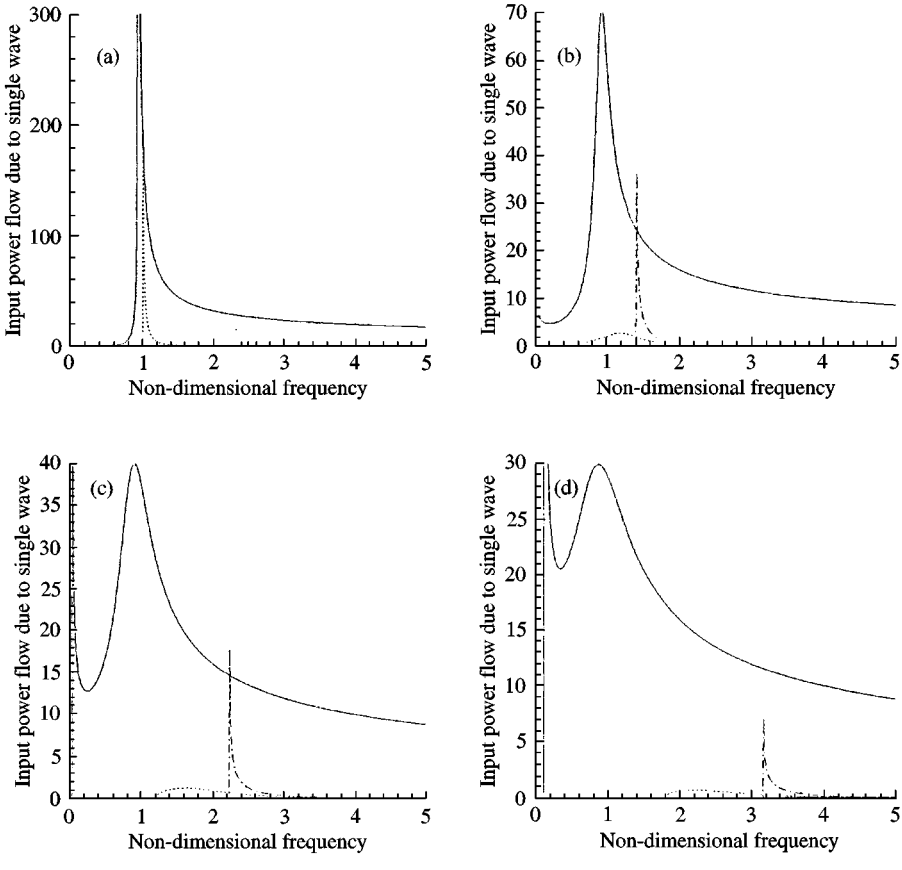

Figure 4. Input power flow due to a single propagating wave into a shell *in vacuo*: (*a*) $n = 0$, (b) $n = 1$, (c) $n = 2$, (d) $n = 3$. ——, $s = 1$; ·····, $s = 2$; – · – · –, $s = 3$.

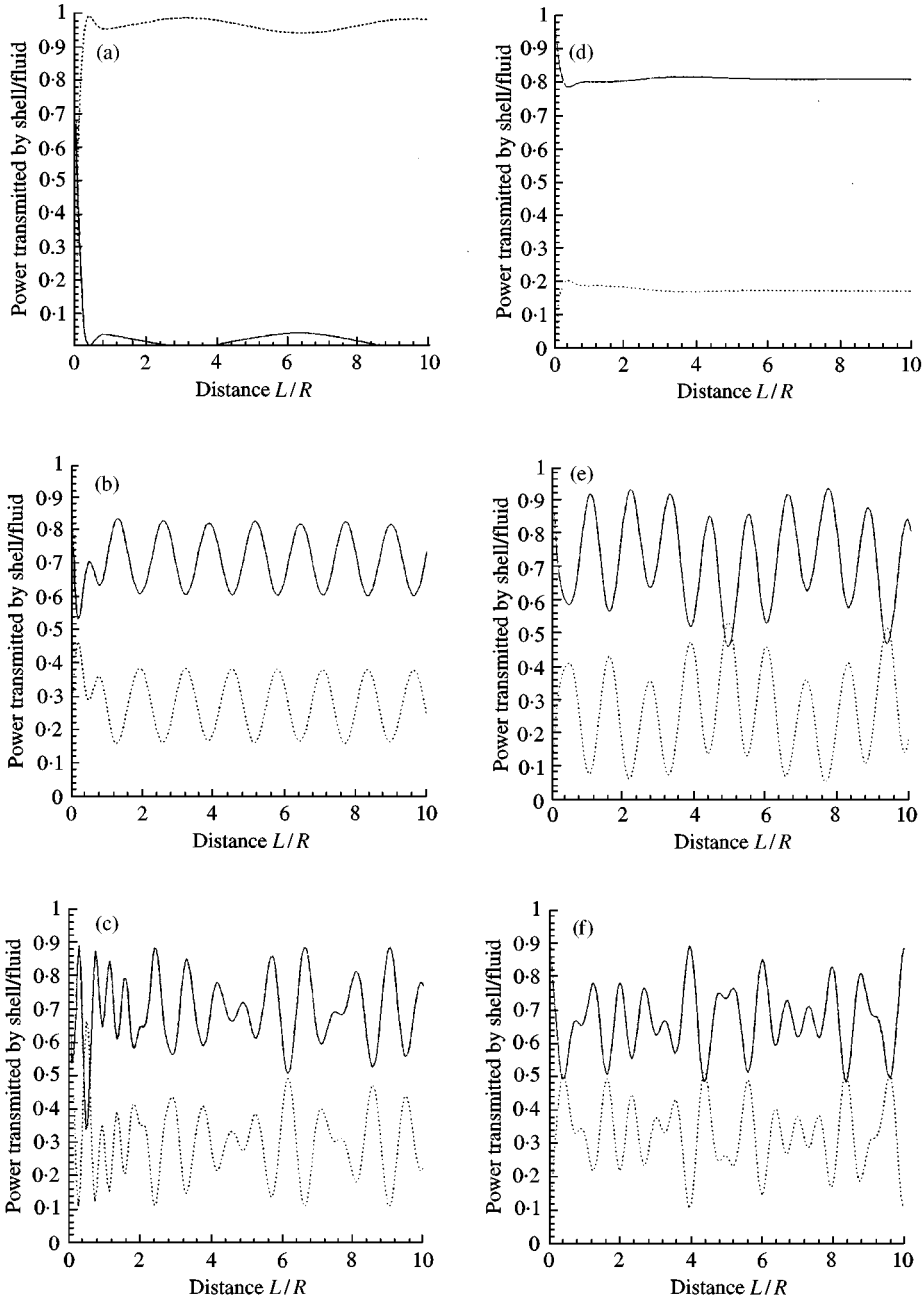

Figure 5. Power flow transmitted by the shell or by the fluid: (a) $n = 0$, $\Omega = 0{\cdot}3$; (b) $n = 0$, $\Omega = 1{\cdot}2$; (c) $n = 0$, $\Omega = 3{\cdot}0$; (d) $n = 1$, $\Omega = 0{\cdot}3$; (e) $n = 1$, $\Omega = 1{\cdot}2$; (f) $n = 1$, $\Omega = 3{\cdot}0$; ——, By the shell; ·····, by the fluid.

propagating wave in the coupled system is fluid type; For circumferential mode order $n = 1$, the difference between P'_{Shell} and P'_{Fluid} is small, which means a strong fluid–shell coupling.

At middle or high frequencies ($\Omega = 1{\cdot}2$ or $3{\cdot}0$), for any circumferential mode order n, both P'_{Shell} and P'_{Fluid} are the "periodic" functions of distance L/R. The reason is that the effect of

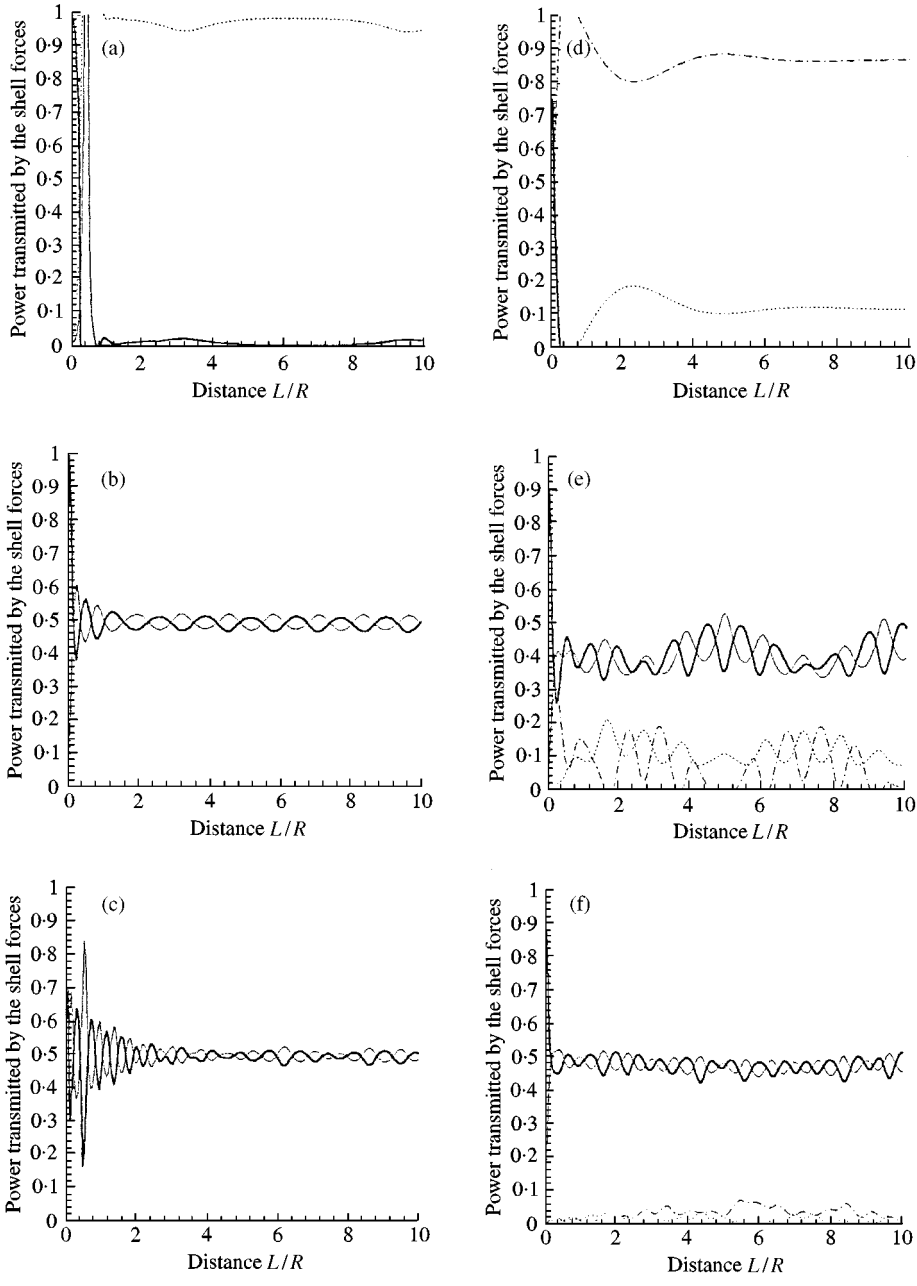

Figure 6. Power flow transmitted by the interanal forces of the shell wall: (a) $n = 0$, $\Omega = 0{\cdot}3$; (b) $n = 0$, $\Omega = 1{\cdot}2$; (c) $n = 0$, $\Omega = 3{\cdot}0$; (d) $n = 1$, $\Omega = 0{\cdot}3$; (e) $n = 1$, $\Omega = 1{\cdot}2$; (f) $n = 1$, $\Omega = 3{\cdot}0$; ·····, P'_N; – · – · –, P'_T; ——, P'_S; ——, P'_M

the attenuated standing waves and the near-field waves is very small and thus the motion of the coupled system changes "periodically" along the shell axial direction.

Figure 6 shows the power flow transmitted by different internal forces (moment) of the shell wall, P'_N, P'_T, P'_S and P'_M plotted against axial distance L/R for the coupled system. The following conclusions can be drawn.

For circumferential mode order $n = 0$ (breathing mode), because the torsional motion is uncoupled with other motions, $P'_{Shell} = P'_N + P'_S + P'_M$. For circumferential mode order $n = 1$ (bending mode), $P'_{Shell} = P'_N + P'_T + P'_S + P'_M$.

At the driving point $L/R = 0$, for any circumferential mode order n and non-dimensional frequencies Ω, $P'_S = 1{\cdot}0$. As L/R increases, P'_S changes into other types of power flow.

At low frequencies ($\Omega = 0{\cdot}3$), for circumferential mode order $n = 0$, $P'_S + P'_M \ll P'_N$, the shell motion is predominately extensional; for circumferential mode order $n = 1$, $P'_S + P'_M \ll P'_N + P'_T$, the motion is mainly in the torsional and extensional directions. At middle and high frequencies ($\Omega = 1{\cdot}2$ or $3{\cdot}0$), for any circumferential mode order n, $P'_S + P'_M \gg P'_N$ and $P'_S + P'_M \gg P'_T$; the motion of the shell wall is mainly in the radial direction. For all frequencies Ω and circumferential mode orders n, $P'_S \approx P'_M$; the power transmitted by the transverse shear force equals that transmitted by the bending moment.

The results for a shell *in vacuo* are given in reference [11]. By comparing the results of a shell filled with fluid with those of a shell *in vacuo*, the following conclusions can be drawn. For a shell *in vacuo*, the variation of power flow transmitted by different forces (moment) of the shell wall is unnoticeable after a distance; for a shell filled with fluid, and middle or high frequencies, the power flow carried by different shell forces (moment) is the "periodic" function of distance L/R, but the variation amplitude is much smaller than that of P'_{Shell} and P'_{Fluid}.

6. CONCLUSIONS

The forced vibration of an infinite elastic circular cylindrical shell filled with fluid is investigated in this paper. By analyzing the vibrational power flow input from an external force and the transmission along the shell axial direction, the following conclusions can be drawn.

(1) The input power flow depends upon the characteristics of free wave propagation to a great extent. The peak frequencies in the input power flow spectrum correspond to the cut-on propagating waves shown in the dispersion curves of the system. Both the residue of near-field waves and that of a pair of attenuated standing waves do not change the input power flow at all. Only those of the propagating waves influence the results of the input power. The input power flow due to different single propagating waves is different. The input power due to the $s = 1$ wave is almost the total power flow for the entire frequency range. The input power flow due to other propagating waves is almost unnoticeable except near its own cut-on frequency and the next one or two propagating waves' cut-on frequencies, where the input power flow is significant.

(2) The power flow transmitted along the shell's axial direction depends greatly upon the characteristics of the free propagating waves. At low frequencies, the variation of different power flows with the distance is slow. For $n = 0$, the power flow in the coupled system is predominantly carried by the motion of fluid; the power flow in the shell all is predominantly carried by the the motion in the axial direction. For $n > 0$, the power flow in the coupled system is mainly carried by the motion of the shell wall and the power in the shell is mainly carried by the motion in the axial and circumferential directions. At middle or high frequencies, the variation of the power flow is large and the power carried by the fluid motion is less than that carried by the shell motion. The power flow carried by different forces (moment) in the shell wall also changes with distance, but the variation amplitudes are much smaller. Most of the power flow in the shell wall is carried by the flexural motion; the power flow carried by the motion in the axial or circumferential direction is unimportant.

ACKNOWLEDGMENTS

The authors are grateful for the financial assistance provided by the National Natural Science Foundation of China (Grant No. 19404005).

REFERENCES

1. V. N. MERKULOV, V. YU, PRIKHODKO and V. V. TYUTEKIN 1979 *Soviet Physics-Acoustics* **25**, 51–54. Normal modes in a thin cylindrical elastic shell filled with fluid and driven by forces specified on its surface.
2. V. N. MERKULOV, V. YU. PRIKHODKO and V. V. TYUTEKIN 1978 *Soviet Physics-Acoustics* **24**, 405–409. Excitation and propagation of normal modes in a thin cylindrical elastic shell filled with fluid.
3. C. R. FULLER and F. J. FAHY 1982 *Journal of Sound and Vibration* **81**, 501–518. Characteristics of wave propagation and energy distributions in cylindrical elastic shells filled with fluid.
4. G. PAVICR 1990 *Journal of Sound and Vibration* **142,** 293–310. Vibrational energy flow in elastic circular cylindrical shells.
5. G. PAVICR 1992 *Journal of Sound and Vibration* **154**, 411–429. Vibroacoustical energy flow through straight pipes.
6. E. G. WILLIAMS 1991 *Journal of Acoustical Society of America* **89**, 1615–1622. Structural intensity in thin cylindrical shells.
7. R. S. LANGLEY 1994 *Journal of Sound and Vibration* **169**, 29–42. Wave motion and energy flow in cylindrical shells.
8. C. R. FULLER 1983 *Journal of Sound and Vibration* **87**, 409–427. The input mobility of an infinite circular cylindrical elastic shell filled with fluid.
9. C. R. FULLER 1986 *Journal of Sound and Vibration* **109**, 259–275. Radiation of sound from an infinite cylindrical elastic shell excited by an internal monopole source.
10. B. J. BREVART and C. R. FULLER 1993 *Journal of Sound and Vibration* **163**, 149–163 Effect of an internal flow on the distribution of vibrational energy in an infinite fluid-filled thin cylindrical elastic shell.
11. X. M. ZHANG and W. H. ZHANG 1990 *Proceedings of ASME PVP*, *Nashville U.S.A*. Vibrational power flow in a cylindrical shell.
12. W. H. ZHANG and X. M. ZHANG 1991 *Proceedings of ASME PVP*, *Atlanta*, *U.S.A*. Vibrational power flow in a cylindrical shell with periodic stiffeners.
13. J. H. JAMES 1982 *Admiralty Marine Technology Establishment*, *Teddington*, *May*. *AMTE*(*N*) *TM*82036, Computation of acoustic power, vibration response and acoustic pressure of fluid-filled pipes.
14. L. FENG 1994 *Journal of Sound and Vibration* **176**, 399–415. Acoustic propagaties of fluid-filled elastic pipes.
15. L. FENG 1995 *Journal of Sound and Vibration* **183**, 169–178. Noise and vibration of a fluid filled elastic pipe coated with an absorptive layer on the inner side of the wall.
16. M. B. XU, X. M. ZHANG 1998 *Journal of Sound and Vibration* **218**, 587–598. Vibration power flow in a fluid-filled cylindrical shell.
17. M. B. XU, X. M. ZHANG and W. H. ZHANG 1999 *Journal of Sound and Vibration*, **224,** 395–410. The effect of wall joint one the vibrational flow propagation in a fluid-filled shell.
18. M. B. XU, X. M. ZHANG and W. H. ZHANG 1999 *Journal of Sound and Vibration* **222**, 531–546. Space-harmonic analysis of input power flow in a periodically stiffened shell filled with fluid.
19. W. FLÜGGE 1973 *Stress in Shells*. New York: Springer-Verlag.
20. M. B. XU 1999 *Ph.D. dissertation*, *Huazhong University of Science and Technology*, Wave propagation and power flow in a cylindrical shell-fluid coupled system.
21. N. W. MCLACHLAN 1934 *Bessel Functions for Engineers*. London: Oxford University Press.
22. P. M. MORSE and K. U. INGARD 1968 *Theoretical Acoustics*. New York: McGraw-Hill.

APPENDIX A: LIST OF SYMBOLS

E	Young's modulus
F	external force

FL	fluid-loading term
h	shell wall thickness
i	$\sqrt{-1}$
$\mathrm{J}_n()$	Bessel function of order n
k_{ns}	axial wavenumber
k_s^r	radial wavenumber
n	circumferential mode number
N, T, S, M	axial force, torsional shear force, transverse shear force and bending moment of the shell wall in the shell axial direction
p_f	pressure in the contained fluid
P_{input}	input power flow
P_{Shell}	power flow transmitted by the shell wall
P_{Fluid}	power flow transmitted by the contained fluid
P_N, P_T, P_S, P_M	power flow carried by the shell force: N, T, S, M
P'	non-dimensional input power flow
R	shell mean radius
s	branch number
u, v, w	shell displacements
U_{ns}, V_{ns}, W_{ns}	shell displacement amplitudes
$\tilde{U}, \tilde{V}, \tilde{W}$	spectral displacements of the shell wall
ρ_f	density of fluid
ρ_s	density of shell
μ	Poisson's ratio
ω	circular frequency
Ω	non-dimensional frequency
λ	non-dimensional axial wavenumber
Φ_{ns}, Ψ_{ns}	characteristic vector
δ	Dirac delta function

Superscripts

*	complex conjugate
′	differentiation